International Journal of Chemistry and Technology

http://dergipark.gov.tr/ijct

Research Article

Flow analyses of highly concentrated xhantan gum fluid

Guler Bengusu TEZEL

ID at end page

Department of Chemical Engineering, Faculty of Engineering and Architecture, Bolu Abant Izzet Baysal University, 14280, Bolu, Turkey

ABSTRACT

The concentration effect of Xanthan gum (XG) solutions (1.0, 1.5, 2.0, 2.5% w/v) on the rheological flow parameters are examined using stress controlled rheometer and gravity driven flow set-up measurement at 25°C. Concentrated XG solutions has yielding behavior obtained by fitting results through Herschel-Bulkley (HB) model with highest regression coefficient $R^2 = 0.995$ and $R^2 = 0.993$ respectively by rheometer and set-up measurement. The results agreed well each other from these measurements. Increasing the concentration of XG solutions promote dynamic and static yield stresses due to increase of entanglement structure density of XG solutions. Also, the magnitudes of consistency index, K, have increasing trend with XG concentration as a result of increasing entanglement density of XG structure. Static yield stress values are much closely dynamic stress values getting from under gravity dynamic flow indicating that supplies undisturbed moleculer structure of XG due to nature of creeping flow.

Keywords: Xanthan Gum, dynamic yield stress, static yield stress, rheometer.

Yüksek derişimli ksantan gam sıvısının akış analizleri

ÖZ

Bu çalışmada, %1.0, %1.5, %2.0, %2.5 w/v derişimine sahip Ksantan gam (XG) sulu çözeltilerinin reolojik akış parametreleri 25°C de stress kontrollü rheometre ve yerçekimi güdümlü akış düzeneği ile incelenmektedir. Akış için eşik streslerine sahip olan yüksek derişimli XG çözeltileri, reometrede $R^2 = 0.995$ ile akış düzeneğinde ise $R^2 = 0.993$ olmak üzere yüksek regresyon katsayıları ile Herscel-Bulkley akış modeline uyum göstermektedir. Ayrıca, her iki deneysel yöntem için sonuçlar birbirleri ile tutarlıdır. XG derişimi arttıkça, XG çözeltisindeki dolanıklık yapı yoğunluğu arttığı için dinamik ve statik eşik stresleri de artmaktadır. Aynı zamanda, viskositenin ölçüsü olan, K, akış paramtresi de artış göstermektedir. Yerçekimi güdümlü akış düzeneği, çok düşük hıza sahip akış sağladığından ve de XG moleküler yapısını bozmadığından durağan eşik stres değerleri, akış düzeneği ölçümlerinden elde edilen dinamik eşik stres değerlerine oldukça yakın bulunmuştur.

Anahtar Kelimeler: Ksantan Gam, dinamik eşik stresi, statik eşik stresi, reometre.

1. INTRODUCTION

For pipe line design considerations of non-Newtonian fluid flows, rheological investigation is a critical issue especially in getting constitutive equatıions for given viscosity information.[1,2] Main difference between Newtonian and non-Newtonian fluids comes from non-linearity relation with shear rate and shear stress data.[3] Hence, viscosity is variable based on applied steady shear rate on the fluid. Using a strain or stress controlled rheometer, the steady shear flow properties of solutions can be measured over a wide range of shear rates.[4] There are many several inelastic and viscoplastic flow models

consisting yield stress parameter to get quantitative evaluation of steady shear flow of non-Newtonian flow models in the literatüre.[5] Bingham, Casson, Herschel-Bulkey models are used frequently to describe the yield and viscosity behaviour of flows.[6] For industrial applications, non-Newtonian fluids have been used widely because of their shear thinning or thickenning rheological properties.[7] Herein, Xanthan gum fluid has been choosen as a non-Newtonian fluid model for the identification of rheological parameters. Xanthan gum (XG) is a naturally occurring polysaccharide consisting primarily chain of glucose.[8] It is used widely as a thickening and stabilizing agent especially in food and

pharmaceutical industries because of high solubility in water, low cost, biodegradable, and non-toxic.[9] Xanthan aqueous solutions have a non-Newtonian rheology, with a shear-thinning and yielding behavior under increasing shear rate. Yielding behavior is related to the hydrogen bridging between xanthan molecules networks when mixed with water due to hydrophilic natüre.[8,9] If the applied stress reaches above the yield stress, entanglement structure is broken down and chains align through the flow generally for yielding fluids as in Figure 1.
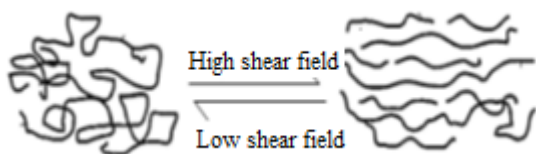

Figure 1. Non-Newtonian structure variation during the flow.

It is expected that entaglement density increases with the increased concentration of the fluid. Applied shear rate or the flow time decides the flow structure. Microstructure and rheology of XG solutions differ with respect to XG concentration. It also produces high viscosity solution with yield stress even at low concentrations.[8] Rheological properties of XG solutions have been performed using dynamic shear tests and small amplitude oscillation test using conventional rheometers.[10,11] However, obtained results from these conventional tests need to be verified with empirical equations.[12,13] Analytical equations are derived from basic momentum conservation equations with pipeline design considerations based on flow profile of flowing fluid.[13,14] The objective of the current study is to investigate the rheological flow properties as dynamic and static yield stress, consistency and flow index of highly concentrated Xanthan solutions using stress controlled rheometer and gravity driven flow set-up.

2. MATERIALS AND METHODS

2.1. Materials

The XG powders were dissolved in distilled water at 25 °C for 6 h using a magnetic stirrer with gentle shaking (400 rpm) in order to prepare 1, 1.5, 2 and 2.5% (w/v) stock solutions of XG. The solutions to be studied were left to stand overnight at 4°C to get complete hydration of XG remove the bubbles of the solutions.

2.2. Rheological and flow measurements

To get flow behavior of XG solutions, dynamic shear tests measurements were performed by a stress

controlled rheometer (Malvern Kinexus Pro, UK) fitted by a cone-and-plate system at 25°C. Diameter and angle of the cone were chosen as 40 mm and 4°, respectively. The gap between the cone-and-plate was fixed at 0.15 mm for all measurements. A peltier plate assembly was used for temperature controlling purpose during the measurements with ±0.1°C precision. Dynamic flow measurements were performed with the supply of gravity driven flow loop as in Figure 2. Test fluid was recirculated using peristaltic pump to move high concentrated XG solutions. Pressure drop was measured at the ends of the pipe with a constant length of 1.50 m using pressure transducer. To get the gravity flow, the storage tank height between 50-100 cm was also adjusted.
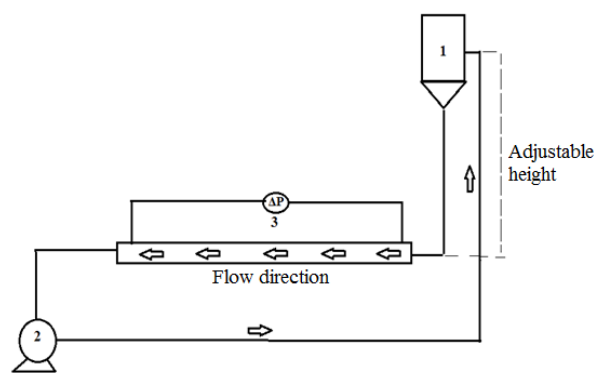

Figure 2. Flow system: 1. Storage tank, 2. Pump 3.Pressure Transducer.

2.3. Theoretical considerations of pipe flow

To evaluate shear viscosity in pipe flow, an incompressible fluid undergoes steady pressure-driven flow. There are many assumptions: laminar flow, no slip on the pipe wall, end effects are negligible.[15,16] The conservation of linear momentum, which equates pressure forces to viscous forces, provides the relationship between the shear stress, σ, and radial position, *r* is as in Eq. (1).

$$\sigma(r) = \frac{-\Delta P r}{2L} \qquad (1)$$

Shear stress at the maximum at the pipe wall, radius *r*, $r = R$, σ_w is written as in Eq. (2);

$$\sigma_w = \frac{-\Delta P R}{2L} \qquad (2)$$

To evaluate the shear rate, volumetric flow rate, *Q* can be given as in Eq. (3);

$$dQ = u 2\pi r dr \qquad (3)$$

Where u is linear velocity at r; the total volumetric rate is found as integration of velocity over the flow area (Eq. (4));

$$Q = -\pi \int_0^{R^2} r^2 du \tag{4}$$

u can be expressed as in Eq. (5) as function of shear stress with changing radius, r ;

$$du = -f(\sigma)dr \tag{5}$$

Where r is $\quad r = \frac{\sigma}{\sigma_w} R \tag{6}$

When Eq. (6) is substituted into Eq. (5), we get Eq. (7);

$$du = -f(\sigma)\frac{R}{\sigma_w}d\sigma$$

$$r^2 = \frac{\sigma^2 R^2}{\sigma_w^2} \tag{7}$$

After mathematically rearrangement, Eq. (8) is obtained as

$$Q = -\pi \int_0^{\sigma_w} \frac{\sigma^2 R^2}{\sigma_w^2}\left(-f(\sigma)\frac{R}{\sigma_w}d\sigma\right)$$

$$\frac{Q}{\pi R^3} = \frac{1}{\sigma_w^3}\int_0^{\sigma_w} \sigma^2 f(\sigma)d\sigma \tag{8}$$

According to rheological measurements, Herschel-Bulkley (HB) model gives best fit as in Eq. (9)

$$\sigma = K(\gamma^n) + \sigma_0$$

$$f(\sigma) = \gamma = \left(\frac{\sigma - \sigma_0}{K}\right)^{1/n} \tag{9}$$

After the substitution Eq. (9) into Eq. (8), Eq. (10) can be written as;

$$\frac{Q}{\pi R^3} = \frac{1}{\sigma_w^3}\int_0^{\sigma_w} \sigma^2 \left(\frac{\sigma - \sigma_0}{K}\right)^{1/n}d\sigma \tag{10}$$

When Eq. (10) is integrated over the wall stress, Eq. (11) gives volumetric flow rate;

$$Q =$$
$$\left(\frac{\pi R^3}{256}\right)\left(\frac{4n}{3n+1}\right)\left(\frac{\sigma_w}{K}\right)^n (1-)^{\frac{1}{n}}\frac{\frac{\sigma_0}{\sigma_w}}{2n+1}[1+\frac{2n}{n+1}\left(\frac{\sigma_0}{\sigma_w}\right)(1+\frac{n\sigma_0}{\sigma_w})]] \tag{11}$$

If the definition of H.B model is;

$$\sigma = K(-\frac{du}{dr})^n + \sigma_0 \tag{12}$$

The velocity profile is also found after integration of Eq. (5) over the radius yields (Eq. (13));

$$u = f(r) = \frac{2L}{\Delta P \left(1 + \frac{1}{n}\right)K^{1/n}}[(\sigma_w - \sigma_0)^{1+\left(\frac{1}{n}\right)}$$

$$-\left(\frac{(\Delta P)r}{2L} - \sigma_0\right)^{1+\left(\frac{1}{n}\right)}] \tag{13}$$

3. RESULTS AND DISCUSSION

3.1. Steady shear measurements

Dynamic shear measurements were carried out using stress controlled rheometer (Malvern Kinexus Pro, UK). Different XG solution with 1.0, 1.5, 2.0, 2.5 w/v % concentration was processed using shear rate ramp measurements. Figure 3 depicts rheological data (shear stress and shear rate) to capture flow behavior of XG solutions over a shear rate range 0.1-100 s^{-1} at 25°C. Plot of shear stress versus shear rate for XG solutions shows non-Newtonian behavior with yield stress due to non-linearity relation between shear stress and shear rate. The apperant shear stress values are increased with increase the XG concentration as expected.
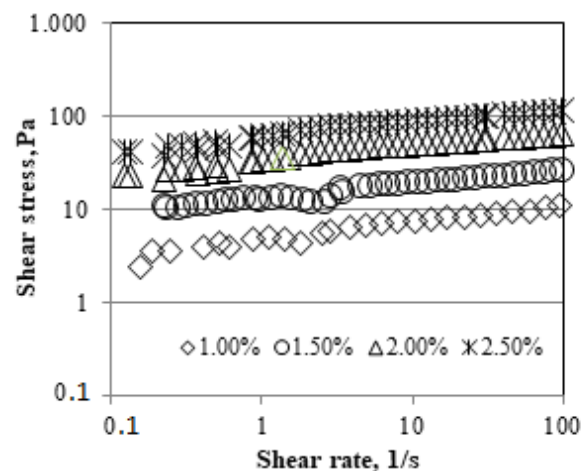

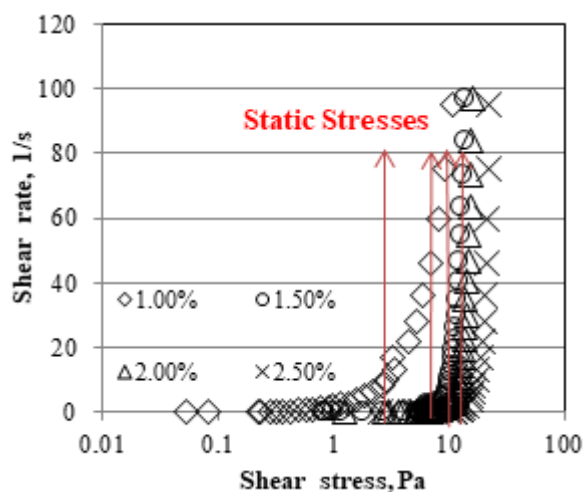**Figure 3.** Experimental shear stress v.s shear rate data.

The results in Figure 3 suggest that steady properties can be modelled by Herschel-Bulkley (HB) model. The rheological model parameters predicted by HB model are listed in Table 1. The coefficient determination (R^2) is in the range of 0.985-0.995. R^2 values show that model perfectly fits to experimental data. Predicted dynamic yield stress rises with increasing XG concentrations.

Flow behavior index, *n* also gives the tendency of shear viscosity changing ratio with respect to shear rate. Lower *n* values at higher XG concentration indicate highly more non-Newtonian and shear thinning behavior of solutions.

Table 1. Fitting flow characteristics of XG solutions using rheometer

XG (w/v%)	Rheometer Measurement Results			
	Dynamic Yield Stress, σ_0 (Pa)	Consistency index, K (Pa.s^n)	Flow index, n	R^2
1.00%	3.842	0.5678	0.264	0.989
1.50%	5.451	1.2451	0.210	0.985
2.00%	7.656	3.2725	0.189	0.992
2.50%	9.852	5.8010	0.164	0.995

The magnitudes of consistency index, *K*, have increasing trend with XG concentration as a result of increasing viscosity of XG solutions. Another important parameter for yielding fluid is static yield stress value. Shear stress ramp results give static yield stress as seen in Figure 4. Static stress is which initiate the flow notations as in Figure 4 and they get higher value than the dynamic stress values as listed in Table 2. These Herschel-Bulkley flow parameters of XG solutions have similar trend as earlier reported by Bobade co-workers[17] They analyzed between the range of 0.3%-0.6% (w/v) of XG solutions. Maximum dynamic yield stress was found as 1.729 Pa for 0.6% of XG solution.

and pressure drop of XG flow and using Equations (11 and 12), wall shear stress and wall shear rate values are derived at the channel wall (r = R). Wall shear stress over wall shear rate gives the viscosity information of XG solutions as seen in Figure 5. For gravity flow of highly concentrated XG solutions,

Table 2. Static yield stresses of XG solutions

XG (w/v%)	Rheometer Measurement Results
	Static Yield Stress (Pa)
1.00%	4.890
1.50%	7.920
2.00%	10.123
2.50%	13.021

Table 3. Fitting flow characteristics of XG solutions using flow set-up

XG (w/v%)	Dynamic Flow Measurement Results			
	Dynamic Yield Stress, σ_0 (Pa)	Consistency index, K (Pa.s^n)	Flow index, n	R^2
1.00%	4.184	0.712	0.277	0.952
1.50%	6845	1.026	0.202	0.982
2.00%	9.865	4.325	0.171	0.992
2.50%	12.108	6.231	0.158	0.993

Figure 4. Static Stresses of XG solutions.

Figure 5. Wall shear stress versus wall shear rate.

3.2. Dynamic flow measurements

In order to investigate the dynamic flow of XG solutions under gravity flow, the flow set-up were used as seen in Figure 2. By measuring volumetric flow rate
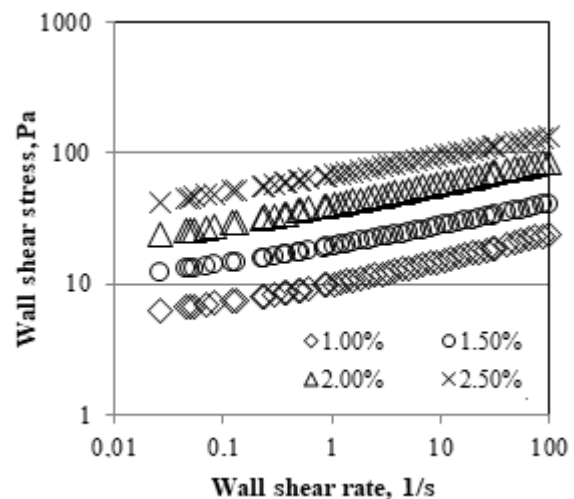
Reynolds number *(Re)* changes the range of order 10^{-7} and 10^{-3} for this flow system. It can be said that it is creeping flow due to *Re* $\ll$ 1. Table 3 shows fitting flow characteristics of XG solutions by using flow set-up. Herein obtained dynamic yield stress values are close to

static ones compared to the rheological results. Static yield stress emerges at the undisturbed fluid situation in such a creeping or very slow flow condisitions. However, during shear test measurements, microstructure of XG solutions can be easily interrupted by increasing shear rates and so dynamic yield stress obtained from rheological measurements has lower values compared to the flow measurements. The flow curves were obtained from Eq. (13). Flow profile or flow field explains the way in which the flow of a fluid behaves or is likely to behave in a pipeline or channel based on its velocity and viscosity. The velocity profiles for the flow of non-Newtonian fluids are given as in Figure 6.
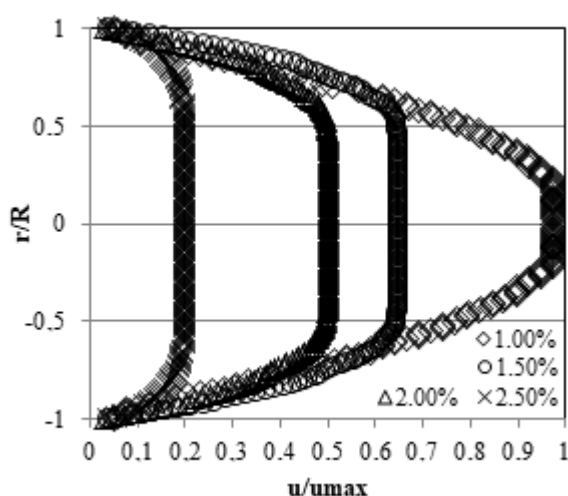
Figure 6. Laminar velocity profile of XG solutions.

These velocity profiles illustrate that with increasing the yield stress enlarges the radius of flowing down the center of pipe due to changing of viscosity variation of XG solutions. Flow profile reaches more plug-flow shape. The slope of flow curves gives the shear rate of the flow. %1 of XG solutions has more velocity changing with respect to radius at channel wall (at r = 1 and r = -1). Hence, maximum wall shear rate is achieved for 1% XG solution. Due to shear thinning nature of XG solutions, as shear rate increases, the viscosity decreases through the center of the channel. Hence, the fluid velocity profile changes over the cross section of the channel. Non-dimensional velocity (u/umax) based on maximum velocity has shifted to lower values as increasing XG solutions owing to more viscous solutions as expected.

4. CONCLUSIONS

Inspection of flow behavior of highly concentrated of XG solutions is analyzed using rheometer and dynamical flow set-up measurements. Dynamic shear stress test and flow measurement results proved that dynamical and static yield stresses increased with concentration which is

an indication of more entanglement of structure of XG. The steady shear and flow experimental results are obtained by Herschel-Bulkley model with high R^2 values. Static yield stress values are found to be higher than dynamic stresses. This may be due to molecular structure deformation of XG during shear tests. On the other hand, flow measurements occurs creeping flow conditions which means undisturbed bulk flow and the dynamic yield results obtained from flow measurements are so close to static those. Further fundamental studies including highly concentrated XG systems in oscillation and creep-relaxation tests with the verification of the experimental measurements will creat a part of future work.

ACKNOWLEDGEMENTS

Conflict of interest

Author declares that there is no a conflict of interest with any person, institute, company, etc.

REFERENCES

1. Barnes, H. A. *J. Non-Newton Fluid* **1997**, 70, 1-33.

2. Barnes, H. A.; Hutton J. F.; Walters, K. *An introduction to rheology*, Elsevier, Amsterdam, 1989.

3. Bird R.B.; Dai G.C.; Yarusso, B. J. Rev. *Chem. Eng.***1983**, 1, 1-83.

4. Tanner, R.I. *Engineering rheology*, 2nd edn. Oxford university press, London, 2000.

5. Barnes, H.A.; Walters, K. *Rheol. Acta* **1985**, .24, 323-326,

6. Chhabra, R.P.; Richardson, J.F. *Non-Newtonian flow and applied rheology,* 2nd edn. Butterworth-Heinemann, Oxford, 2008.

7. Dullaert, K.; Mewis, J. *J. Rheol.* **2005**, 49, 1213-1230.

8. Alquraishi, A.A.; Alsewailem, F.D. *Carbohyd. Polym.* 2012, 88, 859-863.

9. Anna, S. L.; McKinley, G.H. *J. Rheol.* **2001**, 45 (1), 115-138.

10. Cuvelier, G.; Launay, B. *Carbohyd. Polym.* **1986**, 6, 321-333.

11.Lim, T.; Uhl, J. T; Prudhomme, R.K. *J. Rheol.* **1984**, 28, 367-379.

12. Nguyen, Q.D.; Boger, D.V. *Annu. Rev. Fluid* **1992**, 24, 47-88.

13.Yapici, K.; Cakmak, K. N.; Ilhan, N.; Uludag, Y. *Korea-Aust. Rheol. J.* **2014**, 26, 1-9

14. Tozzi, E.J.; Bacca, L.A.; Hartt, W.H.; McCarthy, K.L; McCarthy M. J. *J. Rheol.* **2012**, 56, 1464-1499.

15. Callaghan, P.T. *Rep. Prog. Phys.* **1999**, 62, 599-670.

16. Bird, R.B.; Stewart, W. E.; Lightfoot, E. N. *Transport phenonema*, 1st ed., John Wiley and Sons Inc., New York, USA, 1960.

17. Bobade, V.; Cheetham, M.; Hashim, J.; Eshtiaghi, N. *Water Res.* **2018**, 134, 86-91.

ORCID

0000-0002-0671-208X (G. B. Tezel)